Chapter 2
Advances in Synthesis of Metal Nanocrystals

P. John Thomas, Oliver L. Armstrong, and Sean N. Baxter

2.1 Introduction

Nanomaterials are widely regarded as holding potential answers to challenges in electronics, medicine, biochemistry, environmental and chemical processes areas. Synthetic schemes yielding nanocrystalline metals have reached a certain maturity having witnessed an explosion of interest in the later part of the past 20 years. A rapid change in properties is observed following the reduction in dimensions of the system. In the nanometre size regime, particulates deviate sharply from the properties displayed by their bulk counterparts, as the surface effects become more substantial [1]. The special-scaled size-dependent properties hold from 100s of nm's down to around 1 nm whence individual difference between atomic clusters or nuclei are many and large [2–5]. There is now growing understanding of structure and bonding in clusters [6–8]. In the past year, there is emerging realisation that the footprint of small clusters whose structure is driven by the peculiarities of bonding clearly extends much further than previously believed [8]. In general, polydisperse samples or large particles exhibit an average property that may suffice for certain applications. However, more stringent requirements in terms of size distribution are usually needed for sophisticated applications relying on nanoscopic properties. The characteristics of the whole population, that includes particles of different sizes and properties may interfere with the results and outcomes [9, 10].

There has been much success in obtaining dispersions of nanocrystals with tight control over shape and size. Topical areas include multistep seeded growth processes, post-synthesis size tuning, tailoring the ligand shell for various applications as well as preparing multicomponent alloyed nanocrystals some of which

P.J. Thomas (✉) • O.L. Armstrong • S.N. Baxter
School of Chemistry, Bangor University, LL572UW, Bangor, UK
e-mail: john.thomas@bangor.ac.uk

F.L. Deepak (ed.), *Metal Nanoparticles and Clusters*,
https://doi.org/10.1007/978-3-319-68053-8_2

are multifunctional [9–11]. The expectation of kinetic control over growth schemes tends to entail more nuanced approach to synthesis compared to bulk materials. Modern methods have risen to the challenge producing a bewildering array of choices. The available schemes are far too numerous to be covered in a single chapter or indeed in a whole monograph. At the same time, the nuanced development of each scheme is valuable and mirrors the emerging understanding of nanoscopic materials. Both beginners and seasoned veterans could benefit from a detailed understanding. Hence, in lieu of an overview (with less critical details), this chapter will present a small overview, punctured with more detailed account of select reagents and methods elaborating their course over the years. It is hoped that this would provide sufficient depth and breadth to provide a flavour of the myriad schemes. Synthetic methods not detailed in this chapter include solvothermal synthesis [12] and synthesis in confined medium such as microemulsions [13] and reverse micelles [14].

2.1.1 Nanocrystals in Liquids

Nanoparticulates dispersed or synthesised in the liquid phase are best regarded as colloidal sols with high-optical clarity. A key factor that lends stability to the crystallites is the presence of a ligand shell: a layer of molecular species adorning the surface. Without such protection, the particles tend to aggregate to form bulk species that flocculate or settle down in the medium. Depending on the dispersion medium, the ligands lend stability to particles in two different ways. In an aqueous medium, coulomb interactions between charged ligand species provide a repulsive force to counter the attractive van der Waals force between the tiny grains, by forming an electrical double layer. In an organic medium, the loss of conformational freedom of the ligands as two particles approach each other and the apparent increase in solute concentration provide the necessary repulsive force (see Fig. 2.1). Nanocrystals dispersed in liquids are either charge stabilised or sterically stabilised.

Synthetic schemes are reliant on controlled reduction of dispersed metal salts. The growth of seeds produced following reduction is interrupted by the introduction of a capping agent: a ligand that can bind strongly to low or zero valent surface of nascent crystallites. Reactions typically follow three steps: seeding, growth and termination brought about by binding with a capping agent. Under near-equilibrium growth conditions, Ostwald ripening, a process whereby smaller particles dissolve releasing monomers or ions for consumption by larger particles, tends to widen the size distribution to about 15%. Tight control over sizes is achieved by employing high concentrations of the monomers and capping agents, forcing growth to occur in a transient regime. In practice, seeding, nucleation and termination steps are often not separable, and hence it is common to start with a mixture of metal salts, capping agents and a reducing agent. The relative rates of the steps can be altered by changing parameters such as the concentrations and temperature. This is a popular trick employed to obtain particulates of different dimensions following the same reaction scheme.

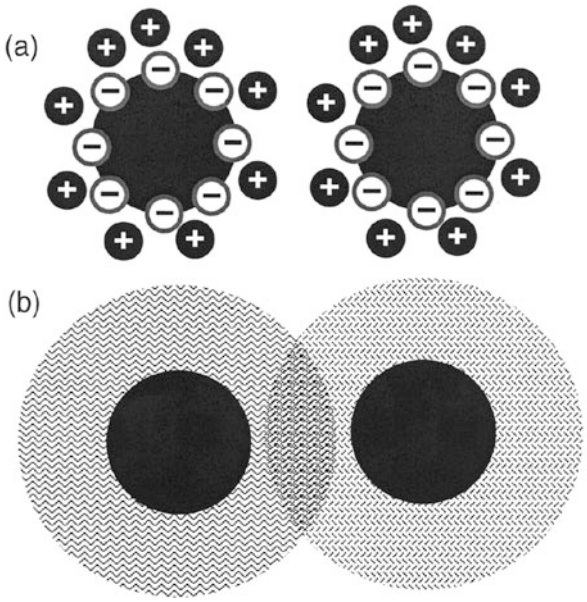

Fig. 2.1 Schematic illustration of two mechanisms stabilising nanocrystals in solution: (**a**) an electric double layer and (**b**) steric stabilisation. In the former, loss of conformational freedom of chain-like ligands provides stability

2.2 Synthesis of Nanocrystals in the Aqueous Phase

Aqueous solvents were a popular medium for the synthesis of nanocrystallites for much of the last century [15]. Hydrosols have been produced with a wide range of reducing agents including common ones such as alcohols, diols, aldehydes, gaseous hydrogen, metal hydrides, diborane and more exotic agents: carbon monoxide, tannic acid [16] and tetrakis(hydroxymethyl)phosphonium chloride. There was a brief of lull in activity in the early noughties, following the discovery of the so-called injection method of synthesis of semiconductor nanocrystals and the Brust method(discussed later). However, the ability of aqueous-based methods to produced shape-controlled nanocrystals as well as potential applications in biochemistry and medicine has led to a revival of interest in recent times.

2.2.1 Sodium Citrate and Related Reducing Agents

This particularly popular method for the synthesis of Ag and Au nanoparticles was first reported by Hauser and Lynn [17] and studied extensively by Turkevich [15] and Frens [18]. Simply adding aq. citrate to a boiling solution of metal chloride resulted in the production of colloidal sols of metals such as Ag, Au, Pt, Pd, bi- and tri-metallic alloys as well [19–21]. The citrate ions act as a reducing agent as well as a capping layer, providing a protective surface covering. The particulates produced are quasi-spherical with large diameters ($>$ 10 nm). The mechanism of

this reduction in the context of nanoparticle synthesis has drawn much attention [22, 23]. Better control over particle dimensions can be exercised by controlling the speciation of the complex ions and the reducing agent. Practically, this is accomplished by changing solution pH [22, 24], solvent [22, 25] and order of addition of the reagents [26]. The use of additional reducing agents such as tannic acid has proved beneficial to obtaining sub-10 nm nanoparticles, and these methods have been christened inverse Turkevich method [16, 27]. Recent advances have led to easy production of sub-10 nm particles of Au and other metals using the citrate method [26, 27]. Current interest is centred on the lability and versatility of the citrate surface layer permitting the functionalization of particles with a wide variety of molecules [28].

2.2.2 Borohydride Reduction

Reduction by borohydride involves the hydrolysis of the borohydride accompanied by the evolution of hydrogen.

$$BH_4^- + 2H_2O \longrightarrow BO_2^- + 4H_2 \tag{2.1}$$

Nanocrystals of a variety of metals such as Au, Ag and Pt have since been made by borohydride reduction [2, 15]. The fast rate of hydrolysis naturally leads to a certain uncertainty in synthesis and necessitates the use of freshly prepared reagent for each run. Further, in some cases, boron may be incorporated in the product [29, 30]. Bönneman and co-workers [31, 32] used triethylborohydrides to avoid the incorporation of boron and have successfully reduced early transition metals such as Ti, Zr, V, Nb and Mb in tetrahydrofuran.

2.2.3 Photochemical Synthesis

Light-induced decomposition of a metal complex or the reduction of metal salts by photogenerated reducing agents such as solvated electrons can be used to prepare nanocrystal. Henglein, Belloni and their co-workers have pioneered the use of photolysis and radiolysis for the preparation of nanoscale metals [33, 34]. Metals highly resistive to reduction such as Cd and Tl have been obtained in colloidal form by photolysis. PVP-covered Au nanocrystals are produced by the reduction of $HAuCl_4$ in formamide by UV irradiation [35]. The reaction is free radical mediated, with the radicals being generated by photodegradation of formamide. Radiolysis of Ag salts in the presence of polyphosphates produces extremely small clusters that are stable in solution for several hours. Effective control can be exercised over the reduction process by controlling the radiation dosage. Radiolysis also provides a means for the simultaneous generation of a larger number of metal nuclei at the

start of the reaction, thereby yielding a fine dispersion of nanocrystals. Studies of the reduction pathways by radiolysis have been carried out [36]. Chaudret and co-workers have prepared hexadecylamine capped indium nanowires using UV light and a cyclopentadienyl complex of indium (In(Cp)) [37].

In 2001, Mirkin and co-workers reported the photoinduced conversion of Ag nanospheres to into distinct nanoprisms [38]. Here, spherical silver particles prepared borohydride reduction of $AgNO_3$ in the presence of sodium citrate and subsequently stabilised by bis(p-sulfonatophenyl)phenylphosphine dihydrate dipotassium were irradiated with a conventional fluorescent light resulting in the spheres transforming into nanoprisms. This report has since spawned a great deal of activity, straddling two topical themes: shape-controlled synthesis [3] and high-quality photochemical tuning [39]. A vivid illustration of the former was reported by the same group which showed that Ag particulates can be coaxed to grow anisotropically through selected excitation of the plasmon (see Fig. 2.2) [40]. Multiphase and sophisticated photochemical control over shape-tuned synthesis is now feasible [41, 42].

2.2.4 Tetrakis(hydroxymethyl)phosphonium Chloride

Tetrakis(hydroxymethyl)phosphonium chloride(THPC) was initially reported in 1921 by Hoffman [43]. Originally unsure, Hoffman later established the accepted structure and synthesised derivatives [44]. During these investigations, it was identified that THPC decomposed in the presence of aqueous alkali hydroxides to form tris(hydroxymethy)phosphine oxide(THPO) as well as formaldehyde and tris(hydroxymethy)phosphine(THP) (Fig. 2.3) [45, 46].

Duff et al. first proposed, in 1993, using THPC as a reducing agent for the reduction of metals, with the added role of stabiliser in aqueous medium [47]. This was developed as a possible replacement for the traditional Faraday synthesis of gold colloids, which employed diethyl ether solutions of white phosphorous [48]. Using THPC, ultrafine gold colloids containing with a mean diameter between 1 and 4 nm, much smaller than the other methods of that time, were successfully produced [47, 49–51].

Two decades later, more extensive studies on the action of THPC in the reduction of metal ions were undertaken [52]. During this study, an overall reaction scheme was proposed, shedding light on the role played by THPC and formaldehyde (Fig. 2.3). Using THPC, it is possible to chemically reduce metal salt precursors, in both aqueous and organic solvents, to successfully obtain metallic nanostructures. It has been shown that nanostructures of gold, silver, palladium, platinum and ruthenium as well as bimetallic and tri-metallic nanostructures can be made [47, 50–56]. Reductions have been carried out in single- and two-phase systems, where the reducing agent and metal precursor are introduced in separate phases [57–59].

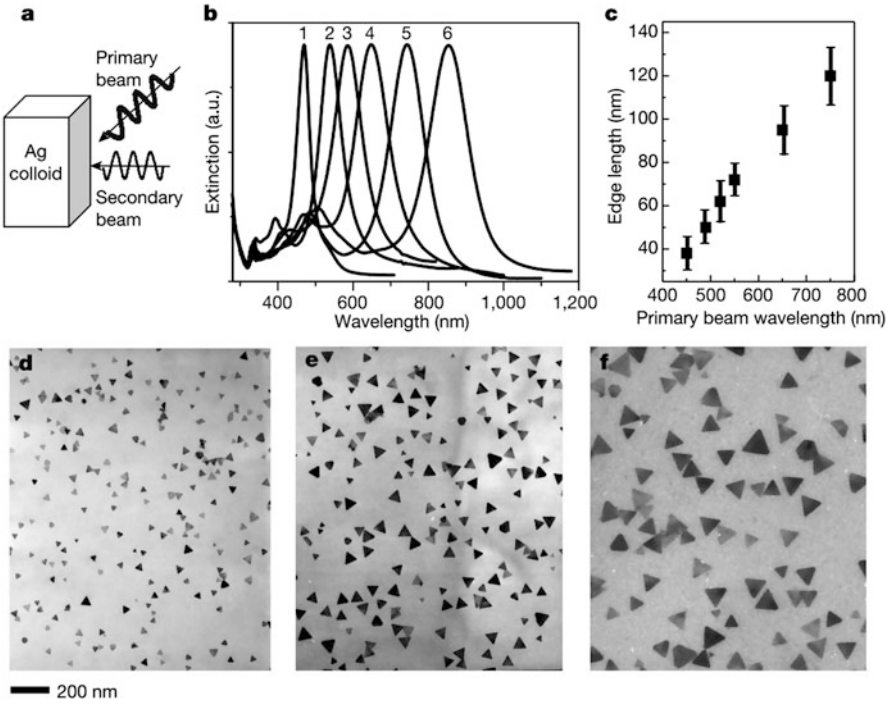

Fig. 2.2 Picture illustrating the controlled of growth of Ag nanospheres into nanoprisms. (**a**) Schematic diagram of dual-beam excitation set-up used to engineer the growth. (**b**) The optical spectra (normalised) for six different-sized nanoprisms (1–6 (approximate) edge length: 38 nm, 50 nm, 62 nm, 72 nm, 95 nm and 120 nm) prepared by varying the primary excitation wavelength (central wavelength at 450, 490, 520, 550, 650 and 750 nm, respectively; width, 40 nm) coupled with a secondary wavelength (340 nm; width, 10 nm). (**c**) The nanoprism edge lengths as a function of the primary excitation wavelength. **d–f** TEM images of Ag nanoprisms with average edge lengths of 38 nm (**d**), 72 nm (**e**) and 120 nm (**f**). Scale bar applies to panels **d–f** (Figure reproduced with permission from Ref. [40])

2.2.4.1 Role of THPC in Reductions

THPC (structure I in Fig. 2.3) converts to THPO (structure III in Fig. 2.3) via THP (structure II in Fig. 2.3) in the presence of hydroxide ions. Formaldehyde and hydrogen are produced during the process [52]. THPO adsorbs onto the surface of nanoparticles as a protecting ligand and quenches nanoparticle growth [56]. Experiments testing the stabilising role of THPC as a ligand, the need for basic hydroxide conditions to activate the reducing power and the influence of formaldehyde have been undertaken by Hueso et al.. Using an aqueous solution of chloroplatinic acid and THPC, it was shown that the reaction did not proceed in the absence of sodium hydroxide. On the addition of formaldehyde, the reaction was able to proceed as normal producing well-crystallised Pt nanoparticles of 1.5 nm diameter. This proved that the THPC freely reacts with hydroxide ions

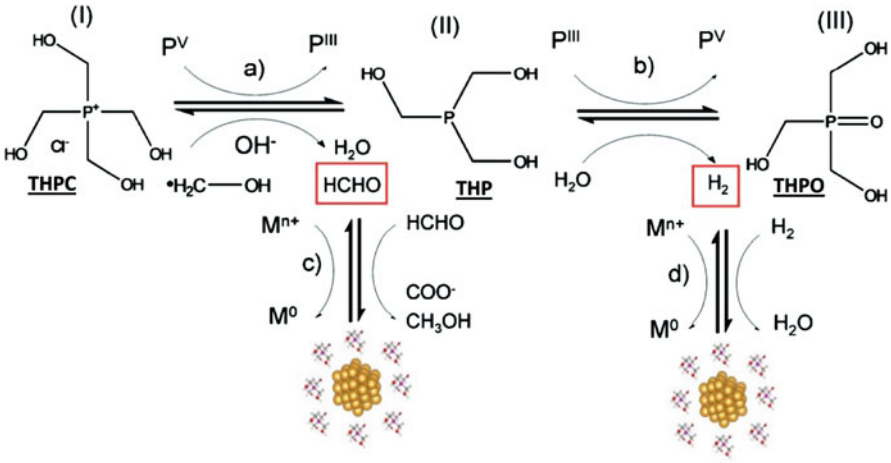

Fig. 2.3 Proposed reaction scheme for the synthesis of metal nanocrystals using THPC and metal salts (Figure reproduced with the permission of the Royal Society of Chemistry from Ref. [52])

generating the formaldehyde, in situ, which can then reduce the metal salts [52]. To test the stabilising role that the THPC played, the reaction was performed in the absence of THPC with formaldehyde employed as the reducing agent. As expected, the reaction occurred generating nanoparticles of Pt; however without the THPC present, interparticle growth and aggregation could occur. This leads to large agglomerates forming as a black precipitate. It was therefore confirmed that THPC acted as both electrostatic stabiliser and generator of formaldehyde through the conversion of THPC to THPO [46, 52, 60]. Hydrogen gas is also produced through the reduction of water by the reaction intermediate (step b in Fig. 2.3). The generated H_2 is then oxidised back to water in the reduction of metal ions [47, 52].

THPC has been utilised in two main methods for the generation of nanoparticles [50, 59]. In a typical one-phase reaction, a metal salt in solution is added to a stirred aqueous mixture of sodium hydroxide and THPC. When using chloroauric acid, the formation of an orange-brown hydrosol of gold nanoparticles of 1–2 nm diameter is noticed [60]. It has been shown that using this method and employing equimolar ratios of chloroplatinic acid and chloroauric acid yielded PtAu alloyed nanoparticles with a mean size of close to 2 nm [52]. Recently Li et al. have utilised THPC in the presence of (±)-α-lipoic acid for the reduction of aqueous $CuSO_4$. THPC produced the more stable nanoparticles when compared to $NaBH_4$ and N_2H_4. In efforts to further increase the capping by the thiolated ligand, dihydrolipoic acid (DHLA), NaCl was later added. TEM analysis of the Cu nanoparticles showed an average diameter of around 1.6 nm [54]. Rao and co-workers have been utilising THPC reduction of metal ions across the toluene-water interface [57, 58, 62–64]. The formation of films of nanoparticles occurs at the interface through a diffusion-controlled process, when metal ions diffusing into the interface interact with reducing agents also in the interface [63]. In this series of reactions metal, salts dissolved in toluene were

carefully layered on top of aqueous NaOH; once the layers had stabilised, THPC was injected into the aqueous phase and reduction proceeded. This method has been used to synthesise gold, silver, copper and palladium. Bi- and tri-metal nanoparticles could also be formed by varying the feed ratios of metal ions in the toluene phase of the reaction [64]. The nanoparticles form as a thin film at the interface which can then be deposited onto a substrate [57] or formed into sol through the addition of a suitable ligand exchange [58]. Typically when using $Au(PPh_3)Cl$, the mean Au nanoparticle diameter after reacting for 24h at room temperature was ≈9 nm, with a close-packed arrangement of nanoparticles separated by an interparticle distance of 1.5 nm. Further studies with $Au(PPh_3)Cl$ have shown that higher temperatures produce larger nanoparticles, 15 nm at 75 °C [61]. The films produced at elevated temperatures, and deposited onto glass substrates, possess relatively fewer cracks and pits than those at cooler temperatures and tend to show higher conductivities in electrical measurements. Higher concentrations of THPC produced less uniform films of nanoparticles with a broader range of diameters. Using highly concentrated precursor, solutions did not affect the distribution of dimensions, merely the quantity of nanoparticles within the expected size range. Ag nanoparticle films produced using $Ag_2(PPh_3)_4Cl_2$ or $Ag(PPh_3)Cl$ in place of the $Au(PPh_3)Cl$ formed highly lustrous interface films with an average diameter of 10 nm [58]. The monometallic 75 °C Ag films showed diameters in the range of 60–100 nm through TEM imaging [64]. When synthesised at room temperature, the Ag films consisted of diameters in the range of 10–50 nm [58]. XPS analysis of pure Ag shows two different Ag species: one of the core Ag and one of the surface Ag bound to the ligands. Studies of silver nanoparticles formed using this method found them to be sensitive to the contact time, temperature and metal ion concentration [62, 63]. Nanoparticle films of Au−Ag, generated at 75 °C, showed an increase from ≈16 nm to ≈60 nm with increasing Ag content, when estimated from XRD peak widths. TEM of the 50:50 bimetal Au−Ag and Au−Cu showed mean diameters of 23.5 nm for Au−Ag and a range 10–25 nm for Au−Cu (Fig. 2.4).

THPC has thus proven to be a versatile reagent for the generation of a number of mono- and bimetallic nanocrystallites, with particularly fine dimensions. Given the current interest in this area, it is anticipated that there would be growing interest in THPC-based reduction.

2.3 Metal Nanocrystals in Nonaqueous Medium

Developments in the vicinity of the turn of the century have led to the nonaqueous medium emerging as a powerful alternative. Crucial early reports that helped established such schemes include the Brust method and the preparation of Fe-Pt nanocrystals by a combination of reduction and thermolysis in a single pot. In general, nonaqueous routes provide greater control over the course of the reaction.

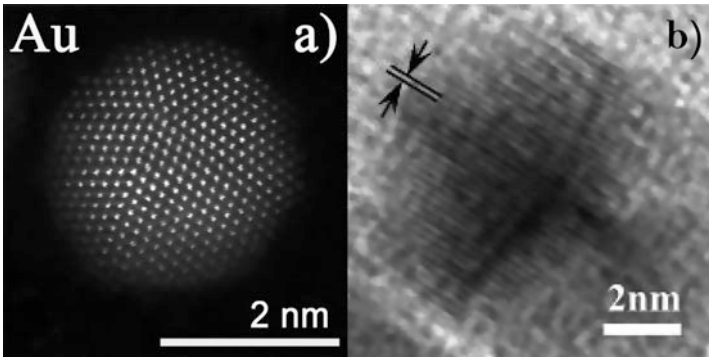

Fig. 2.4 STEM (**a**) and HRTEM (**b**) of Au nanoparticles synthesised in the THPC method as a hydrosol (**a**) and water-toluene interface (**b**). The films of nanoparticles formed at the interface were deposited onto substrates and used directly (Figure adapted from Refs. [52, 61] with permission from the Royal Society of Chemistry and American Chemical Society. Copyright 2005 American Chemical Society)

2.3.1 Brust Method

A two-phase borohydride reduction-based scheme to prepare Au nanocrystals reported by Schiffrin and co-workers [65] has emerged as one of the most popular methods for synthesis of Au nanocrystals [2, 66, 67]. Here, aqueous Au ions are transferred to a toluene layer using tetraoctylammonium bromide, a phase transfer catalyst which is also capable of acting as a stabilising agent. The Au complex now in toluene is reacted with alkanethiols to form polymeric thiolates. Aqueous borohydride is added to the reaction vessel to effect reduction. The capping action of the thiols is related to the formation of a crystalline monolayer on the metal particle surface [68, 69]. The powerful capping action of alkanethiols at metal particle surfaces prompted Murray [70] to name these particles monolayer-protected clusters (MPC). In practice, it is possible to dry the dispersion of particulates and re-disperse the dried form back into liquid by introducing the "solvent". The length of the alkyl chain and the concentration of borohydride influence the size of the nanocrystals. This method has been successfully extended to prepare MPCs of Pt, Ag and Pd as well [2, 66, 71–73].

2.3.2 Thermolysis Routes

Historically, organometallic routes to metal nanocrystals were employed for the preparation of ferrofluids [74]. Cobalt particles have been prepared by decomposition of low-valent $Co_2(CO)_8$ dicobalt octacarbonyl, in an inert atmosphere, in the presence of surface ligands [75, 76]. Carbonyl complexes are noted for the

clean decompositions at high temperatures (over 200 °C) yielding just the metal and gaseous CO. This sort of clean break-up is not dissimilar to the needs of the chemical vapour deposition (CVD)-based process, and indeed initial routes borrowed heavily from the better established CVD methods. For example, the Fischer group have prepared Cu nanocrystals by thermolysis of a CVD precursor, $[Cu(OCH(Me)CH_2NMe_2)_2]$ in both trialkylphosphines and long-chain amines medium [77].

By carrying out thermolysis reactions in high-boiling solvents in the presence of capping agents, nanocrystals of various materials are obtained. The critical role played by surfactants was graphically illustrated in the case of ϵ-Co [78, 79]. Building on previous successes in injection-based organometallic synthesis of CdSe nanocrystals, Bawendi and co-workers sought to produce Co. They found that in the presence of tri-n-octylphosphine oxide (TOPO), the reduction of the carbonyl in a high-boiling solvent butylbenzene, a new and previously unknown phase of Co, christened ϵ-Co was obtained. This form has lower density, but comparable magnetic moment as the fcc(α) and hcp(β) forms. Crucially, in the absence of TOPO, the fcc form was obtained. Thermal decomposition provides remarkable control over size and is well suited for scale up to gramme quantities. Indeed, Hyeon and co-workers have reported the synthesis of gramme-scale quantities of Fe and Co nanocrystals by thermolysis of metal-oleate complexes in high-boiling solvents [80, 81]. Decomposition of low-valent organic compounds could also be brought about by other means. One of the early reports concerns the sonochemical decomposition of iron pentacarbonyl in the presence of surface capping agents, such as oleic acid or polyvinylpyrrolidone(PVP) [82].

In the organic phase, reducing agents like lithiumtriethylborohydride ($LiBEt_3H$, also called superhydride) can be used to mimic the reduction chemistry prevalent in the aqueous phase. For example, Co chloride in a solvent mixture consisting of oleic acid and an alkylphosphine Sun and Murray [83] has been reduced to obtain Co nanocrystals. Here, alkylphosphine serves as a capping agent as well. Liz-Marzan and co-workers have pioneered the synthesis of a number of nanocrystallites using dimethylformamaide as reducing agent [84].

2.3.2.1 Bimetallic and Other Systems

As mentioned previously, bimetallic nanocrystals can usually be generated by employing a mixture of monometallic precursors. Sun and co-workers, in an effort to create nanocrystals of the magnetic material Fe-Pt, uncovered a whole new paradigm in the organometallic synthesis of metal nanocrystals [85]. To obtain suitably alloyed particles, both iron and platinum nuclei need to be generated simultaneously, presenting a substantial challenge due to the extreme difference in reduction potential between the two metal ions. Here, platinum acetylacetonate ($Pt(acac)_2$) was reduced by a long-chain dialcohol (polyol-type process, discussed later), whilst iron pentacarbonyl was decomposed thermolytically, both in the presence of oleic acid and a long-chain amine. This elegant combination of

reduction and thermolysis in a one-pot reaction has sparked huge interest and led to more advanced synthetic schemes [86, 87]. The original route itself was improved by replacing iron pentacarbonyl with iron(II) chloride, followed by high-temperature reduction using superhydride [86]. This modification gave greater control over the Fe:Pt ratio in nanocrystallites. Other magnetic nanocrystals such as $CrPt_3$ [88] and CoPt [89] have been obtained following this route. The original report by Sun helped bring the role of seeding into focus.

2.4 Digestive Ripening

Digestive ripening provides a simple, low-temperature process by which shape, size and composition of noble metal nanocrystals can be altered by heating in the presence of a surface active reagent that allows exchange of metal atoms between metals of differently sized nanoparticles resulting in a more monodisperse product [10, 90–92]. This process also has an advantage over size separation methods for gaining a monodisperse sample as the former results in waste material, whereas in the latter, the total mass of metal atoms is divided into equally sized particulates.

This process was pioneered by Klaubunde and others from the late 1990s. The mechanistic properties of the process have not fully been uncovered, but a number of controlled studies have attempted to provide an accurate description for the process [9, 10, 93–95].

There have been a number of models showing how digestive ripening can produce a monodisperse product and the process by which two metals may alloy from a polydisperse binary mixture to a monodispersed alloy colloid [90, 93, 94, 96]. These studies indicate that size and number of particles (concentration) are critical to obtain size focusing. Experimental results with bulk Au powders appear to agree with these predictions [96].

Digestive ripening occurs in complete contrast to the better understood phenomena of Ostwald ripening where over a period of time, particle size in a polydisperse colloid increases as the smaller particles are sacrificed to aid the growth of larger particles, ultimately leading to a single large particle [91, 93]. The process of Ostwald ripening is directed by a reduction in interface free energy, producing fewer particles with the progress of the reaction [94]. Digestive ripening works by a different mechanism whereby the smallest particles in solution grow at the expense of the larger particles [90, 91].

The breakdown of larger particles is aided and abetted by a digestive ripening agent that extracts material from larger particles back into solution to then be used to grow the smaller particles equally. The process is shown schematically in Fig. 2.5 resulting in a highly ordered superlattice of monodisperse particles. As digestive ripening is at odds to Ostwald ripening, another factor must be present in the reaction to counter any reduction in interface free energy and force a resulting increase in particle number. Of the two potential driving forces, electrostatic and strain, the latter is thought more likely as in the case of solid particles in a liquid

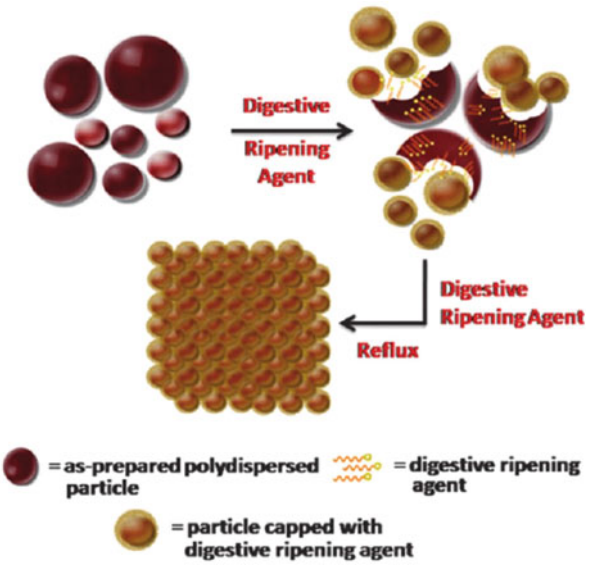

Fig. 2.5 Diagram showing the role of digestive ripening agent in the process (Figure reproduced with permission from [10])

medium; the former is likely to be minuscule [97, 98] In addition to extracting ions from surfaces, the digestive ripening agents also act as simple surfactants placing themselves between the solid particles and the liquid phase thereby reducing the interfacial free energy allowing for easier transfer of metal ions through solution from the larger particles to the smaller. It has been shown that many various reagents with different ligand groups can be effectively employed [10, 99–101].

The choice of which surfactant to use in the process of digestive ripening must be based on the desired size of particle to be attained, as each agent yields particles of specific dimensions. This is due to a myriad of factors with each ligand influencing the interfacial free energy to different extent due to steric properties, electrostatic charges and other energies. The ripening agents can be loosely placed in groups based on the moiety that has most affinity to the metal being processed, e.g. amine, silanes and phosphines. These surfactants usually have a highly electronegative atom or group of atoms with typically a methyl chain. Further, the solvent must be carefully chosen to help the ripening agent act as a surfactant.

As was mentioned previously, much early work was by Klaubunde et al. where digestive ripening was demonstrated as a homogenising process for Au and Ag nanoparticles, turning polydisperse colloids with diameters in the range of 2–40 nm to monodisperse systems with controlled dimensions between 4 and 5 nm [102]. Much recent attention has been placed on using digestive ripening as a process by which to alloy noble metal nanoparticles, now the addition of a secondary metal ion. Such modification may throw up issues that were not present when ripening just one metal. As such metals of a similar composure are typically used to minimise these problems, things are made simpler if just one digestive ripening agent/surfactant

can be used or similar experimental conditions such as temperature and solvent are utilised for the two metals [9, 90, 93, 97].

The introduction of two digestive ripening agents has not had as much attention. The use of more than one may result in size-focused particles, but with the possibility of two or more distinct populations, the process could completely fail in its aim to reduce polydispersity. When mixing two metals in solution and employing the digestive ripening technique to produce an alloy, it has often been found that a small or negligible reduction of particle sizes is often found over the whole sample population, this points to the proposed mechanism of surfactants reducing the interfacial tensions of the largest particles in the sample, releasing small atomic clusters or ions into solution to attach to smaller particles growing on the established crystal structures [90, 103]. The overall reduction in size points to a total increase in number of particles. The optical properties of the produced alloy particles can easily be monitored by UV/Vis during the reaction, as it has been seen that over the length of the procedure, two discrete absorption peaks for each metal will shift towards each other and integrate into one peak when the process of alloying is complete [90, 97].

SEM and TEM images of particles produced in this method provide data of average sizes of a large sample population, these particles are often formed into superlattices of regular distribution partially due to the monodispersity. These images are also of importance when working with alloys or core/shell morphologies, as it can be seen the alloys tend to have excellent atomic ordering within the particle with no areas of contrasting density [90, 93, 103]. This points to the uniform mixing of atomic-level components throughout all particles.

Size focusing, digestive ripening or inverse Ostwald ripening has thus allowed for precisely controlled production of a range of noble metal and other metal particles and their corresponding alloys. Adopting a variety of metals and digestive ripening agents, this method has shown that it is possible to create monodisperse nanoparticle populations of a set size and can conceivably also provide routes for synthesising other metal particles.

2.5 Nanostructures with Structural Anisotropy and High-Energy Facets

The past decade has seen rapid growth in routes to anisotropic nanostructures, particularly nanorods of precious metals such as Au and Ag [104–106]. Facets of such nanostructures are nearly always made up of open, high-index planes [3, 107, 108]. In the conventional crystal growth scheme, the high-index planes naturally grow to extinction; however, the nature of anisotropic nanocrystals requires that certain facets consist of open planes. The mechanisms underpinning anisotropic growth remain unclear despite a burgeoning portfolio of synthetic schemes. Clearly, kinetic control and engineering of the growth process are important. The current schemes are mainly based in aqueous solvents with the polyol method (discussed later) being

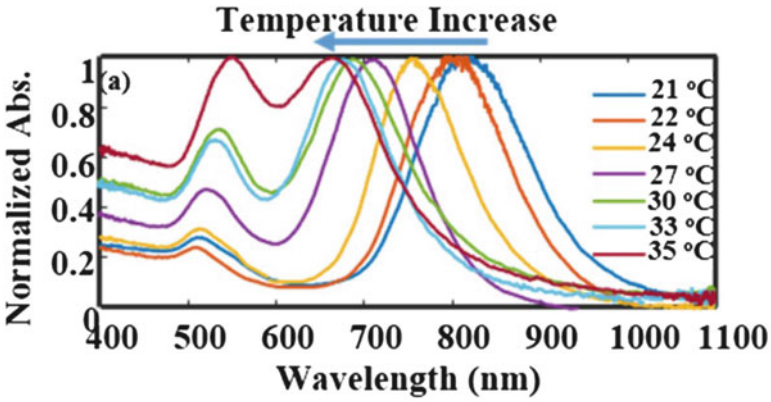

Fig. 2.6 The absorption spectra of Au nanorods of different aspect ratios by varying the growth temperature. The temperatures are indicated. The length of the nanorods increases from approximately 21 to 35 nm at the rate of 3.5 nm/°C. Simultaneously, the diameter of the rods increases starting from approximately 21 at the rate of 3.5 nm/°C (Reproduced with permission from [117]. Copyright 2017 American Chemical Society)

the main nonaqueous route. Fervent effort is currently underway to uncover growth mechanisms and to devise reliable routes. For example, there is much excitement surrounding recent success in synthesising gramme-scale quantities of nanorods [109] and other shapes [110]. The main methods of anisotropic growth include seed-mediated growth, selective etching of certain facets by foreign ions (halides) and growth in anisotropic templates. Some of these schemes produce nanorods and other anisotropic structures by oriented attachments of nanocrystals [111].

Nanorods of Au and other anisotropic structures possess a number of attractive features with potential applications in areas such as sensing, imaging, medicine, electronics, spectroscopy and data storage [112]. For example, spherical Au particulates exhibit a single peak due to surface plasmon resonance, but nanorods with two different axes (the longitudinal and transverse) exhibit two distinct plasmon resonances (see Fig. 2.6). The position of the longitudinal plasmon band is influenced by the aspect ratio of the nanorod [113, 114]. In addition to exciting applications, the plasmon band provides a quick and easy probe to ascertain the characteristics of nanorods. The ends of nanorods have a chemistry distinct from the other parts, permitting selective reactions at the ends including ones aimed at directing self-assembly [115, 116].

The history of seed-mediated methods can be traced all the way back to Zsigmondy's efforts in 1917 [118]. Current methods involve the separation of nucleation and growth steps, often involving two distinct reaction schemes. Hence, great control can be exercised over the growth including the use of seeds of one metal to grow anisotropic structure of a different metal. The revival of interest in this area has been aided to a great deal by efforts of the Murphy group [104, 105]. Topical studies repeatedly emphasise that subtle variations in the growth conditions

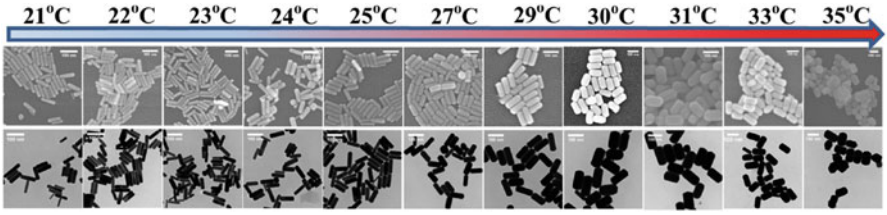

Fig. 2.7 SEM (*top*) and TEM (*bottom*) images of the Au nanorods synthesised at different temperatures. The scale bar corresponds to 100 nm (Reproduced with permission from [117]. Copyright 2017 American Chemical Society)

such as pH, temperature [117] and concentrations can impart dramatic differences in anisotropy of the product (see Fig. 2.7) [97, 98, 104, 108].

Underpotential deposition is an important process that underpins the formation of nanostructures with high-index facets and anisotropic structures [107, 108]. This process has been well studied in the case of noble metal surfaces and electrodes [119]. Here, a layer of a metal such as Ni is deposited on the surface of another (say Pd) at significantly lower potential than the bulk reduction. This is primarily because the initial Pd-Ni bond can in some circumstances be stronger than Ni-Ni bonds. Surfaces decorated with adlayers can slow or in some cases completely stop growing. Underpotential deposition upsets the delicate balance of growth rates that result in isotropic forms. In some cases, the adlayers may act as trigger points for easy nucleation of the other metal facilitating energetically favourable heterogeneous nucleation. The latter is the likely case for the seeded growth of core-shell particulates.

Isotropic evolution of morphology may also be interrupted by oxidative etching [107]. Surface atoms can be oxidised and potentially redispersed in solution by oxidative etchants such as Br^-, Fe^{3+}, O_2/Cl and NH_4OH/H_2O_2. For example, Pd nanorods have been obtained by a kinetically controlled growth scheme mediated by etching Br^- ions [120].

2.5.1 Silver Nanowires Synthesised by the Polyol Process

The polyol process is a well-documented process for producing finely divided particles of noble and related metals and was pioneered by Fievet et al. in the late 1980s [121–124]. In early studies, particles of Co, Ni, Cu, Au, Ag and their alloys in the size range of 100 nm to a few microns have been obtained by this method [125, 126]. Here, ethylene glycol is used as both the solvent in which the metal salts and other precursors are dissolved and as the reducing agent in the system [127, 128]. The glycol permits the use of temperatures as high as 190 °C. This higher temperature than aqueous systems allows for noble metal structures to be formed. Polyvinylpyrrolidone(PVP) is often used to protect the crystallites. This is

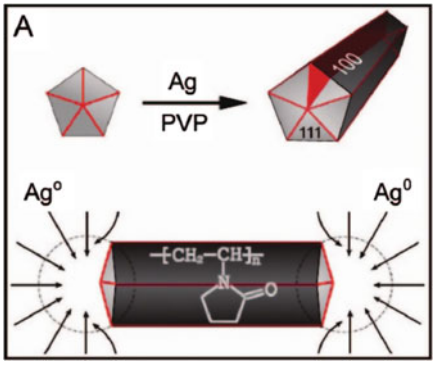

Fig. 2.8 Diagram showing how PVP preferentially protects the (100) crystal face of Ag nanowires (Reproduced with permission of the American Chemical Society from [124]. Copyright 2007 American Chemical Society)

particularly important in the case of magnetic particulates to prevent aggregation (Fig. 2.8).

It is now believed that ethylene glycol degrades under heat to yield glycoaldehyde which reduces the metal salts. In early experiments, it was thought that in situ generated acetaldehyde was the reducing agent as diacetyl was detected in the final solution [121, 122, 129, 130]. This is likely true in this case but is probably a side product from the initial reduction of the cobalt and nickel hydroxide precursors used, promoting acetaldehyde production from the presence of as formed hydroxide ions. As such it is now thought that glycoaldehyde is a common in situ reducing agent alongside EG itself responsible for many polyol syntheses of Ag nanostructures [123, 124, 129].

Controlled growth in these conditions occur in either in three steps in a one-pot reaction or in two steps when using pre-synthesised seeds on which to grow. In the case of a one-pot synthesis, the reaction starts with the metal salt/salts being reduced to form small clusters from metal atoms and ions, secondly these nuclei or small clusters will become seeds with defined crystal structures and faces that can be monitored, and thirdly the seeds will be directed to grow in certain planes giving distinct morphologies [124, 131]. At each step, there is a combination of thermodynamic and kinetic factors that must be considered, and any slight change in any one factor can result in particles of different shapes being formed. The formation of specific shapes or morphologies from this method is not fully understood due to the lack of experimental tools available to show the mechanism of seed formation from small atomic clusters or ions in situ [124, 131, 132].

The use of seeds is common for this method where near to monodisperse seeds are made prior in a separate reaction and then added into the polyol system to provide a crystalline structure with defined crystal faces on which to grow with further in situ produced small atomic clusters and ions [128, 131, 133, 134]. These pre-synthesised seeds do not necessarily need to be of the same metal of as the desired product but do form a constituent part of the final particles [128, 134]. Commonly used seeds for the process of forming silver nanowires are Ag, Cu or Pt and are made in relatively easy syntheses with high control over dispersity.

Copper and Pt reagents are commonly added to the reaction and have been found to not only act as seeds but also to facilitate and increase the rate of the reaction. The work of Korte et al. describes the oxygen-scavenging properties of added CuCl or $CuCl_2$ in the polyol process whereby Cu^+ is reduced by the solvent and reducing agent EG to its Cu^{2+} state. The Cu^{2+} then scavenges any adsorbed oxygen from the (111) face of the silver oxidising to Cu^+. The EG can keep reducing the Cu^+ back to Cu^{2+} providing a constant etching of oxygen from the Ag surface allowing the nanowires to grow faster [135]. The addition of Fe species has been studied in a similar way to CuCl and $CuCl_2$ as way of etching adsorbed oxygen from the (111) face of silver due to the (100) face being protected by PVP or other surfactant. It is not required that pre-synthesised seeds or oxygen-scavenging reagents are used but they can greatly increase the yield and reduce the dispersity of the product [133, 136, 137].

Due to the sensitivity of this reaction to multiple variables, temperature of the reaction must be tightly controlled to try and limit variations in the shape and size of the produced particles. Reports detail a drop-by-drop addition of reagents to the reaction vessel, so as to not dramatically reduce the overall temperature of the reaction. Typical injection rates vary between 1 and 50 ml/hr in an attempt to keep the reaction balanced between thermodynamic and kinetic forces [138]. It has been demonstrated that changing the reaction temperature by 5–10 °C affects the shape, size and dispersity of the obtained particles [128, 138]. A highly monodisperse product is often desired and is obtainable by using slow injection to mitigate temperature drop [132].

In a typical reaction, as a first step, a portion of EG is heated to the reaction temperature. In the case of Ag nanorod synthesis, this tends to be around 160–170 °C, but for metals with higher reduction potentials, higher temperatures up to 190 °C can be accessed with ethylene glycol. The reflux apparatus is set up to ensure minimal evaporation of solvent over the reaction time. The solvent helps to elevate temperature for a whilst prior to adding additional reagents [124, 136, 137]. Some reports have had success with adding in the PVP at this early stage, whereas others inject the PVP solution simultaneously with the metal salt solutions. In the second step, low concentrations (or lower than that of PVP concentration) of metal precursors in EG are added dropwise to the heated reaction vessel. The introduction of the salt such as $AgNO_3$ dropwise yields Ag^+ ions that condense to form small nuclei with as yet undefined crystal structure. The seeds are capable of acquiring different bulk-like close-packed forms depending on the reaction conditions and the energetics of certain structures. It is has been suggested that the nanowire structures can only form from seeds with a multiply twinned decahedral structure rather than just a single-crystal fcc structure, so this ability for the small nuclei to form and remove such defects in situ is important for this process [133]. As the nuclei grow, they become irrevocably attached to a certain crystal structure as the energy required to convert to another form is too costly. These can now be considered seeds for further crystal growth as their structure will not now change [124, 131, 139].

The next stage of crystal growth involves the structures growing mostly in just one dimension to form the nanowires; an important part in this stage is the presence

of PVP. It is understood that PVP is a capping agent in this process and will preferentially bind to any (100) facets of Ag over the (111) facets which are left bare and this is where the next crystal growth occurs with Ag^+ ions binding to the ends and conforming to the defined crystal structure from the seed particle [131, 140, 141]. This process is understood to progress by Ostwald ripening with larger ready formed particles growing at the expense of smaller nuclei particles and free metal ions [128, 134, 138]. The presence of PVP as mentioned before allows the silver crystals to grow in just on dimension [132].

The reaction is often said to be monitored by colour, where upon initial addition of $AgNO_3$ the solution turns slightly yellow, indicating the production of small silver nanocrystal seeds. As the reaction continues, the solution should turn more to a grey-silver colour and over the reaction time will become more thick, wispy and turbid, which is the accepted visual confirmation of the formation of nanowires [136–138]. The reaction is often left at reaction temperature for around an hour after all reagents have been added; as the final stage progresses by Ostwald ripening, this just allows more time for the nanowires to form [131].

Some reports indicate a product yield of 90–95% nanowires, but this often involves the use of pre-synthesised seeds, with slightly lower yields having been gained from methods that do not use seeds. A common technique for separating the nanowires from any other formed nanocrystals is by centrifugation, as the nanowires are much harder to disperse in solvents such as acetone and ethanol than any much smaller nanocrystals formed in this reaction, the supernatant can be removed after centrifugation removing any extraneous ions, reactants and unwanted nanocrystals [137, 138, 142].

2.6 Conclusions

These are clearly exciting times for nanomaterial synthesis. The ability to synthesize high-quality materials with great control over size, shape, composition and structural properties is promising to usher in the next generation of applications. The evermore sophisticated schemes though are not underpinned by an understanding of the underlying mechanism. We await clarity in this regard. We envisage that progress in this area will continue to be driven by curiosity as well as motivated by real world applications of which there are plenty.

References

1. C.N.R. Rao, G.U. Kulkarni, P.J. Thomas, P.P. Edwards, Size-dependent chemistry: properties of nanocrystals. Chem. A Eur. J. **8**(1), 28–35 (2002)
2. M.-C. Daniel, D. Astruc, Chem. Rev. **104**, 293–346 (2004)
3. C. Burda, X. Chen, R. Narayanan, M.A. El-Sayed, Chem. Rev. **105**, 1025–1102 (2005)
4. J. Scholl, A.L. Koh, J. Dionne, Nature **483**, 421–427 (2012)
5. E. Roduner, Chem. Soc. Rev. **35**, 583–592 (2006)

6. Y. Lu, W. Chen, Sub-nanometre sized metal clusters: from synthetic challenges to the unique property discoveries. Chem. Soc. Rev. **41**(9), 3594–3623 (2012)
7. R. Jin, C. Zeng, M. Zhou, Y. Chen, Atomically precise colloidal metal nanoclusters and nanoparticles: Fundamentals and opportunities. Chem. Rev **116**(18), 10346–10413 (2016)
8. I. Chakraborty, T. Pradeep, Atomically precise clusters of noble metals: emerging link between atoms and nanoparticles. Chem. Rev. **117**, 8208–8271 (2017)
9. S.P. Bhaskar, B.R. Jagirdar, J. Chem. Sci. **124**, 1175–1180 (2012)
10. D.S. Sidhaye, B.L.V. Prasad, New J. Chem. **35**, 755–763 (2011)
11. B.L.V. Prasad, C.M. Sorensen, K.J. Klabunde, Chem. Soc. Rev. **37**, 1871–1883 (2008)
12. J. Lai, W. Niu, R. Luque, G. Xu, Solvothermal synthesis of metal nanocrystals and their applications. Nano Today **10**, 240–267 (2015)
13. A.K. Ganguli, A. Ganguly, S. Vaidya, Microemulsion-based synthesis of nanocrystalline materials. Chem. Soc. Rev. **39**(2), 474–485 (2010)
14. M.-P. Pileni, The role of soft colloidal templates in controlling the size and shape of inorganic nanocrystals. Nat. Mater. **2**(3), 145 (2003)
15. J. Turkevich, P.C. Stevenson, J. Hillier, A study of the nucleation and growth processes in the synthesis of colloidal gold. Discuss. Faraday Soc. **11**, 55 (1951)
16. T. Ahmad, Reviewing the tannic acid mediated synthesis of metal nanoparticles. J. Nanotechnol. **2014**, 954206 (2014)
17. E.A. Hauser, J.E. Lynn, *Experiments in Colloid Chemistry* (McGraw-Hill, New York/London, 1940)
18. G. Frens, Controlled nucleation for regulation of particle-size in monodisperse gold suspensions. Nat. Phys. Sci. **241**, 20 (1973)
19. D.N. Furlong, A. Launikonis, W.H.F. Sasse, J.V. Sanders, Colloidal platinum sols. preparation, characterization and stability towards salt. J. Chem. Soc. Faraday Trans. 1 **80**, 571 (1984)
20. A. Harriman, G.R. Millward, P. Neta, M.C. Richoux, J.M. Thomas, Interfacial electron-transfer reactions between platinum colloids and reducing radicals in aqueous solution. J. Phys. Chem. **92**(5), 1286–1290 (1988)
21. R.S. Miner, S. Namba, J. Turkevich, in *Proceedings of the 7th International Congress on Catalysis*, Kodansha, 1981
22. X. Ji, X. Song, J. Li, Y. Bai, W. Yang, X. Peng, Size control of gold nanocrystals in citrate reduction: the third role of citrate. J. Am. Chem. Soc. **129**(45), 13939–13948 (2007)
23. J. Kimling, M. Maier, B. Okenve, V. Kotaidis, H. Ballot, A. Plech, Turkevich method for gold nanoparticle synthesis revisited. J. Phys. Chem. B **110**(32), 15700–15707 (2006)
24. F. Schulz, T. Homolka, N.G. Bastús, V. Puntes, H. Weller, T. Vossmeyer, Little adjustments significantly improve the Turkevich synthesis of gold nanoparticles. Langmuir **30**, 10779 (2014)
25. I. Ojea-Jimenez, F.M. Romero, N.G. Bastus, V. Puntes, Small gold nanoparticles synthesized with sodium citrate and heavy water: Insights into the reaction mechanism. J. Phys. Chem. C **114**, 1800–1804 (2010)
26. S.K. Sivaraman, S. Kumar, V. Santhanam, Monodisperse sub10 nm gold nanoparticles by reversing the order of addition in Turkevich method – the role of chloroauric acid. J. Coll. Inter. Sci. **361**, 543–547 (2011)
27. J. Piella, N.G. Bastús, V. Puntes, Size-controlled synthesis of sub-10-nanometer citrate-stabilized gold nanoparticles and related optical properties. Chem. Mater. **28**(4), 1066–1075 (2016)
28. N.G. Bastus, E. Sanchez-Tillo, S. Pujals, C. Farrera, C. Lopez, E. Giralt, A. Celada, J. Lloberas, V. Puntes, Homogeneous conjugation of peptides onto gold nanoparticles enhances macrophage response. ACS Nano **3**, 1335–1344 (2009)
29. G.N. Glavee, K.J. Klabunde, C.M. Sorensen, G.C. Hadjipanayis, Borohydride reduction of cobalt ions in water. Chemistry leading to nanoscale metal, boride, or borate particles. Langmuir **9**(1), 162–169 (1993)
30. G.N. Glavee, K.J. Klabunde, C.M. Sorensen, G.C. Hadjipanayis, Sodium borohydride reduction of cobalt ions in nonaqueous media. formation of ultrafine particles (nanoscale) of cobalt metal. Inorg. Chem. **32**(4), 474–477 (1993)

31. H. Bönnemann, W. Brijoux, R. Brinkmann, T. Joußen, B. Korall, E. Dinjus, Formation of colloidal transition metals in organic phases and their application in catalysis. Angew. Chem. Int. Ed. **30**(10), 1312–1314 (1991)
32. H. Bo, W. Brijoux, R. Brinkmann, E. Dinjus, R. Fretzen, T. Joußen, B. Korall, et al., Highly dispersed metal clusters and colloids for the preparation of active liquid-phase hydrogenation catalysts. J. Mol. catal. **74**(1–3), 323–333 (1992)
33. J. Belloni, M. Mostafavi, Radiation-induced metal clusters. Nucleation mechanism and chemistry, in *Metal Clusters in Chemistry*, vol. 3, ed. by P. Braunstein, L.A. Oro, P.R. Raithby (Wiley, Weinheim, 1999), pp. 1213–1244
34. J. Belloni, Nucleation, growth and properties of nanoclusters studied by radiation chemistry: application to catalysis. Catal. Today **113**(3), 141–156 (2006)
35. M.Y. Han, L. Zhou, C.H. Quek, S.F.Y. Li, W. Huang, Room temperature coulomb staircase on pure and uniform surface-capped gold nanoparticles. Chem. Phys. Lett. **287**(1), 47–52 (1998)
36. Z.S. Pillai, P.V. Kamat, What factors control the size and shape of silver nanoparticles in the citrate ion reduction method? J. Phys. Chem. B **108**(3), 945–951 (2004)
37. K. Soulantica, A. Maisonnat, F. Senocq, M.-C. Fromen, M.-J. Casanove, B. Chaudret, Angew. Chem. Int. Ed. **40**, 2984 (2001)
38. R. Jin, Y.W. Cao, C.A. Mirkin, K.L. Kelly, G.C. Schatz, J.G. Zheng, Photoinduced conversion of silver nanospheres to nanoprisms. Science **294**(5548), 1901–1903 (2001)
39. S. Linic, U. Aslam, C. Boerigter, M. Morabito, Photochemical transformations on plasmonic metal nanoparticles. Nat. Mater. **14**(6), 567 (2015)
40. R. Jin, Y.C. Cao, E. Hao, G.S. Matraux et al., Controlling anisotropic nanoparticle growth through plasmon excitation. Nature **425**(6957), 487 (2003)
41. C. Burda, X. Chen, R. Narayanan, M.A. El-Sayed, Chemistry and properties of nanocrystals of different shapes. Chem. Rev. **105**(4), 1025–1102 (2005)
42. A. Abedini, A.A.A Bakar, F. Larki, P.S. Menon, M.S. Islam, S. Shaari, Recent advances in shape-controlled synthesis of noble metal nanoparticles by radiolysis route. Nanoscale Res. Lett. **11**(1), 287 (2016)
43. A. Hoffman, The action of hydrogen phosphide on formaldehyde. J. Am. Chem. Soc. **43**(7), 1684–1688 (1921)
44. A. Hoffman, The action of hydrogen phosphide on formaldehyde. II. J. Am. Chem. Soc. **52**(7), 2995–2998 (1930)
45. W.J. Vullo, Studies concerning the neutralization of tetrakis (hydroxymethyl) phosphonium chloride and the reaction of tris (hydroxymethyl) phosphine with formaldehyde. J. Org. Chem. **V**(9), 9–11 (1968)
46. W.A. Reeves, J.D. Guthrie, Intermediate for flame-resistant polymers – reactions of tetrakis(hydroxymethyl)phosphonium chloride. Ind. Eng. Chem. **48**(1), 64–67 (1956)
47. D.G. Duff, A. Baiker, P.P. Edwards, A new hydrosol of gold clusters. 1. Formation and particle size variation. Langmuir **9**(9), 2301–2309 (1993)
48. M. Faraday, The Bakerian lecture: experimental relations of gold (and other metals) to light. Philos. Trans. R. Soc. Lond. **147**(0), 145–181 (1857)
49. D.G. Duff, A. Baiker, P.P. Edwards, A new hydrosol of gold clusters. J. Chem. Soc. Chem. Commun. **272**(1), 96 (1993)
50. W.W. Bryan, A.C. Jamison, P. Chinwangso, S. Rittikulsittichai, T.-C. Lee, T R Lee, Preparation of THPC-generated silver, platinum, and palladium nanoparticles and their use in the synthesis of Ag, Pt, Pd, and Pt/Ag nanoshells. RSC Adv. **6**(72), 68150–68159 (2016)
51. P.J. Thomas, G.U. Kulkarni, C.N.R. Rao, Dip-pen lithography using aqueous metal nanocrystal dispersions. J. Mater. Chem., **14**, 625–628 (2004)
52. J.L. Hueso, V. Sebastián, Á. Mayoral, L. Usón, M. Arruebo, J. Santamaría, Beyond gold: rediscovering tetrakis-(hydroxymethyl)-phosphonium chloride (THPC) as an effective agent for the synthesis of ultra-small noble metal nanoparticles and Pt-containing nanoalloys. RSC Adv. **3**(26), 10427 (2013)
53. M.K. Sanyal, V.V. Agrawal, M.K. Bera, K.P. Kalyanikutty, J. Daillant, C. Blot, S. Kubowicz, O. Konovalov, C.N.R. Rao, Formation and ordering of gold nanoparticles at the toluene–water interface. J. Phys. Chem. C **112**(6), 1739–1743 (2008)

54. D. Li, Z. Chen, Z. Wan, T. Yang, H. Wang, X. Mei, One-pot development of water soluble copper nanoclusters with red emission and aggregation induced fluorescence enhancement. RSC Adv. **6**(41), 34090–34095 (2016)
55. G. Hofmann, G. Tofighi, G. Rinke, S. Baier, A. Ewinger, A. Urban, A. Wenka, S. Heideker, A. Jahn, R. Dittmeyer, J.-D. Grunwaldt, A microfluidic device for the investigation of rapid gold nanoparticle formation in continuous turbulent flow. J. Phys. Conf. Ser. **712**, 012072 (2016)
56. L. Usón, V. Sebastian, A. Mayoral, J.L. Hueso, A. Eguizabal, M. Arruebo, J. Santamaria, Spontaneous formation of Au-Pt alloyed nanoparticles using pure nano-counterparts as starters: a ligand and size dependent process. Nanoscale **7**(22), 10152–10161 (2015)
57. G.L. Stansfield, P.V. Vanitha, H.M. Johnston, D. Fan, H. AlQahtani, L. Hague, M. Grell, P.J. Thomas, Growth of nanocrystals and thin films at the water-oil interface. Philos. Trans. A. Math. Phys. Eng. Sci. **368**(1927), 4313–30 (2010)
58. C.N.R. Rao, G.U. Kulkarni, P.J. Thomas, V.V. Agrawal, P. Saravanan, Films of metal nanocrystals formed at aqueous–organic interfaces. J. Phys. Chem. B **107**(30), 7391–7395 (2003)
59. P.J. Thomas, E. Mbufu, P. O'Brien, Thin films of metals, metal chalcogenides and oxides deposited at the water–oil interface using molecular precursors. Chem. Commun. **49**(2), 118–127 (2013)
60. D.G. Duff, A. Baiker, I. Gameson, P.P. Edwards, A new hydrosol of gold clusters. 2. A comparison of some different measurement techniques. Langmuir **9**(9), 2310–2317 (1993)
61. V.V. Agrawal, G.U. Kulkarni, C.N.R. Rao, Nature and properties of ultrathin nanocrystalline gold films formed at the organic–aqueous interface. J. Phys. Chem. B **109**(15), 7300–7305 (2005)
62. C.N.R. Rao, K.P. Kalyanikutty, The liquid-liquid interface as a medium to generate nanocrystalline films of inorganic materials. Acc. Chem. Res. **41**(4), 489–499 (2008)
63. R. Krishnaswamy, S. Majumdar, R. Ganapathy, V.V. Agrawal, A.K. Sood, C.N.R. Rao, Interfacial rheology of an ultrathin nanocrystalline film formed at the liquid/liquid interface. Langmuir **23**(6), 3084–3087 (2007)
64. V.V. Agrawal, P. Mahalakshmi, G.U. Kulkarni, C.N.R. Rao, Nanocrystalline films of Au–Ag, Au–Cu, and Au–Ag–Cu alloys formed at the organic–aqueous interface. Langmuir **22**(4), 1846–1851 (2006)
65. M. Brust, M. Walker, D. Bethell, D.J. Schiffrin, R. Whyman, Synthesis of thiol-derivatised gold nanoparticles in a two-phase liquid–liquid system. J. Chem. Soc. Chem. Commun. 801–802 (1994)
66. M. Brust, C.J. Kiely, Some recent advances in nanostructure preparation from gold and silver particles: a short topical review. Colloids Surf. A Physicochem. Eng. Asp. **202**(2), 175–186 (2002)
67. P. Huang, J. Lin, Z. Li, H. Hu, K. Wang, G. Gao, R. He, D. Cui, A general strategy for metallic nanocrystals synthesis in organic medium. Chem. Commun. **46**(26), 4800–4802 (2010)
68. R.G. Nuzzo, D.L. Allara, Adsorption of bifunctional organic disulfides on gold surfaces. J. Am. Chem. Soc. **105**(13), 4481–4483 (1983)
69. Y. Xia, G.M. Whitesides, Soft lithography. Annu. Rev. Mater. Sci. **28**(1), 153–184 (1998)
70. R.W. Murray, M.J. Hostetler, J.J. Stokes, Langmuir **12**, 3604 (1996)
71. J.R. Heath, C.M. Knobler, D.V. Leff, Pressure/temperature phase diagrams and superlattices of organically functionalized metal nanocrystal monolayers: the influence of particle size, size distribution, and surface passivant. J. Phys. Chem. B **101**(2), 189–197 (1997)
72. B.A. Korgel, S. Fullam, S. Connolly, D. Fitzmaurice, Assembly and self-organization of silver nanocrystal superlattices: ordered "soft spheres". J. Phys. Chem. B **102**(43), 8379–8388 (1998)
73. S. Chen, K. Huang, J.A. Stearns, Alkanethiolate-protected palladium nanoparticles. Chem. Mater. **12**(2), 540–547 (2000)
74. M. Green, Organometallic based strategies for metal nanocrystal synthesis. Chem. Commun. **2005**, 3002–3011 (2005)

75. M.P. Pileni, Adv. Funct. Mater. **11**, 323 (2001)
76. E. Papirer, P. Horny, H. Balard, R. Anthore, C. Petipas, A. Martinet, J. Colloid Interface Sci. **94**, 220 (1983)
77. J. Hambrock, R. Becker, A. Birkner, J. Weiss, R.A. Fischer, Chem. Commun. 68 (2002)
78. D.P. Dinega, M.G. Bawendi, Angew. Chem. Int. Ed. **38**, 1788 (1999)
79. V.F. Puntes, K.M. Krishnan, A.P. Alivisatos, Science **291**, 2115 (2001)
80. J. Park, K. An, Y. Hwang, J.-G. Park, N. Han-Jin, K. Jae-Young, J.-H. Park, N.-M. Hwang, T. Hyeon, Ultra-large-scale syntheses of monodisperse nanocrystals. Nat. Mater. **3**(12), 891 (2004)
81. J. Park, J. Joo, S. Gu Kwon, Y. Jang, T. Hyeon, Synthesis of monodisperse spherical nanocrystals. Angew. Chem. Int. Ed. **46**, 4630–4660, (2007)
82. K.S. Suslick, M. Fang, T. Hyeon, J. Am. Chem. Soc. **118**, 11960 (1996)
83. S. Sun, C.B. Murray, Synthesis of monodisperse cobalt nanocrystals and their assembly into magnetic superlattices. J. Appl. Phys. **85**(8), 4325–4330 (1999)
84. I. Pastoriza-Santos, L.M. Liz-Marzan, Pure Appl. Chem. **72**(6957), 83–90 (2000)
85. S. Sun, C.B. Murray, D. Weller, L. Folks, A. Moser, Monodisperse fept nanoparticles and ferromagnetic fept nanocrystal superlattices. Science **287**, 1989–1992 (1999)
86. S. Sun, S. Anders, T. Thomson, J.E.E. Baglin, M.F. Toney, H.F. Hamann, C.B. Murray, B.D. Terris, J. Phys. Chem. B **107**, 5419 (2003)
87. A.-H. Lu, E.L. Salabas, F. Schueth, Magnetic nanoparticles: synthesis, protection, functionalization, and application. Angew. Chem. Intl. Ed. **46**(8), 1222–1244 (2007)
88. A. Tomou, I. Panagiotopoulos, V. Tzitzios, W. Li, G.C. Hadjipanayis, Chemical synthesis and L1(2) ordering of CrPt3 nanoparticles. J. Mag. Mag. Mater. **334**, 107–110 (2013)
89. J. Tuaillon-Combes, E. Bernstein, O. Boisron, P. Melinon, Alloying effect in copt nanoparticles probed by x-ray photoemission spectroscopy: validity of the bulk phase diagram. J. Phys. Chem. C **114**(31), 13168–13175 (2010)
90. A.B. Smetana, K.J. Klabunde, C.M. Sorensen, A.A. Ponce, B. Mwale, J. Phys. Chem. B **110**, 2155–2158 (2006)
91. P. Sahu, B.L.V. Prasad, Langmuir **30**, 10143–10150 (2014)
92. J.R. Shimpi, D.S. Sidhaye, B.L.V. Prasad, Digestive ripening: a fine chemical machining process on the nanoscale. Langmuir **33**, 9491–9507 null (2017) PMID:28562058
93. D.K. Lee, N.M. Hwang, Scr. Mater. **61**, 304–307 (2009)
94. N.-M. Hwang, J.-S. Jung, D.-K. Lee, Thermodynamics and kinetics in the synthesis of monodisperse nanoparticles, in *Thermodynamics – Fundamentals and Its Application in Science*, ed. by R. Morales-Rodriguez (InTech, Rijeka, 2012)
95. J.A. Manzanares, P. Peljo, H.H. Girault, Understanding digestive ripening of ligand-stabilized, charged metal nanoparticles. J. Phys. Chem. C **121**(24), 13405–13411 (2017)
96. D.K. Lee, S.I. Park, J.K. Lee, N.M. Hwang, Acta Mater. **55**, 5281–5288 (2007)
97. Y. Ji, S. Yang, S. Guo, X. Song, B. Ding, Z. Yang, Colloids Surf. A Physicochem. Eng. Asp. **372**, 204–209 (2010)
98. M.L. Lin, F. Yang, J.S. Peng, S. Lee, J. Appl. Phys. **115**, 1–8 (2014)
99. B.L.V. Prasad, S.I. Stoeva, C.M. Sorensen, K.J. Klabunde, Chem. Mater. **15**, 935–942 (2003)
100. P. Sahu, J. Shimpi, H.J. Lee, T.R. Lee, B.L.V. Prasad, Langmuir, **33**, 1943–1950 (2017)
101. P. Sahu, B.L.V. Prasad, Chem. Phys. Lett. **525–526**, 101–104 (2012)
102. X.M. Lin, C.M. Sorensen, K.J. Klabunde, J. Nanoparticle Res. **2**, 157–164 (2000)
103. Y. Yang, X. Gong, H. Zeng, L. Zhang, X. Zhang, C. Zou, S. Huang, J. Phys. Chem. C **114**, 256–264 (2010)
104. N.D. Burrows, A.M. Vartanian, N.S. Abadeer, E.M. Grzincic, L.M. Jacob, W. Lin, J. Li, J.M. Dennison, J.G. Hinman, C.J. Murphy, Anisotropic nanoparticles and anisotropic surface chemistry. J. Phys. Chem. Lett. **7**(4), 632–641 (2016)
105. C.J. Murphy, T.K. Sau, A.M. Gole, C.J. Orendorff, J. Gao, L. Gou, S.E. Hunyadi, T. Li, Anisotropic metal nanoparticles: synthesis, assembly, and optical applications. J. Phys. Chem. B **109**, 13857–13870 (2005)

106. A. Ruditskiy, H.-C. Peng, Y. Xia, Shape-controlled metal nanocrystals for heterogeneous catalysis. Annu. Rev. Chem. Biomol. Eng. **7**, 327–348 (2016)
107. L. Zhang, W. Niu, G. Xu, Synthesis and applications of noble metal nanocrystals with high-energy facets. Nano Today **7**(6), 586–605 (2012)
108. M. Grzelczak, J. Pérez-Juste, P. Mulvaney, L.M. Liz-Marzán. Shape control in gold nanoparticle synthesis. Chem. Soc. Rev. **37**(9), 1783–1791 (2008)
109. K. Park, M.-S. Hsiao, Y.-J. Yi, S. Izor, H. Koerner, A. Jawaid, R.A. Vaia, Highly concentrated seed-mediated synthesis of monodispersed gold nanorods. ACS Appl. Mater. Interfaces **9**, 26363–26371 (2017)
110. A. Klinkova, E.M. Larin, E. Prince, E.H. Sargent, E. Kumacheva, Large-scale synthesis of metal nanocrystals in aqueous suspensions. Chem. Mater. **28**(9), 3196–3202 (2016)
111. Q. Zhang, S.-J. Liu, S.-H. Yu, Recent advances in oriented attachment growth and synthesis of functional materials: concept, evidence, mechanism, and future. J. Mater. Chem. **19**(2), 191–207 (2009)
112. E.C. Dreaden, A.M. Alkilany, X. Huang, C.J. Murphy, M.A. El-Sayed, The golden age: gold nanoparticles for biomedicine. Chem. Soc. Rev. **41**(7), 2740–2779 (2012)
113. S. Link, M.B. Mohamed, M.A. El-Sayed, Simulation of the optical absorption spectra of gold nanorods as a function of their aspect ratio and the effect of the medium dielectric constant. J. Phys. Chem. B **103**(16), 3073–3077 (1999)
114. C. Noguez, Surface plasmons on metal nanoparticles: the influence of shape and physical environment. J. Phys. Chem. C **111**(10), 3806–3819 (2007)
115. T. Mokari, E. Rothenberg, I. Popov, R. Costi, U. Banin, Selective growth of metal tips onto semiconductor quantum rods and tetrapods. Science **304**(5678), 1787–1790 (2004)
116. P. Liu, R. Qin, G. Fu, N. Zheng, Surface coordination chemistry of metal nanomaterials. J. Am. Chem. Soc. **139**(6), 2122–2131 (2017) PMID:28085260
117. X. Liu, Y. Jingwen, J. Luo, X. Duan, Y. Yao, T. Liu, The effect of growth temperature on tailoring the size and aspect ratio of gold nanorods. Langmuir **33**, 7479–7485 (2017)
118. R. Zsigmondy, Die keimmethode zur herstellung kolloider metallösungen bestimmter eigenschaften. Zeitschrift für anorganische und allgemeine Chemie, **99**(1), 105–117 (1917)
119. V. Sudha, M.V. Sangaranarayanan, Underpotential deposition of metals: structural and thermodynamic considerations. J. Phys. Chem. B **106**(10), 2699–2707 (2002)
120. Y. Xiong, H. Cai, B.J. Wiley, J. Wang, M.J. Kim, Y. Xia, Synthesis and mechanistic study of palladium nanobars and nanorods. J. Am. Chem. Soc. **129**(12), 3665–3675 (2007)
121. F. Fievet, J.P. Lagier, M. Figlarz, MRS Bull. **14**, 29–34 (1989)
122. F. Fievet, J.P. Lagier, B. Blin, B. Beaudoin, M. Figlarz, Solid State Ionics **32–33**, 198–205 (1989)
123. F. Bonet, K. Tekaia-Elhsissen, K.V. Sarathy, Bull. Mater. Sci. **23**, 165–168 (2000)
124. B. Wiley, Y. Sun, Y. Xia, Acc. Chem. Res. **40**, 1067–1076 (2007)
125. R. Seshadri, C.N.R. Rao, Preparation of monodispersed, submicron gold particles. Mater. Res. Bull. **29**(7), 795–799 (1994)
126. P. Saravanan, T.A. Jose, P.J. Thomas, G.U. Kulkarni, Submicron particles of co, ni and co-ni alloys. Bull. Mater. Sci. **24**(5), 515–521 (2001)
127. Q.N. Luu, J.M. Doorn, M.T. Berry, C. Jiang, C. Lin, P.S. May, J. Colloid Interface Sci. **356**, 151–158 (2011)
128. Y. Sun, Y. Yin, B. T. Mayers, T. Herricks, Y. Xia, Chem. Mater. **14**, 4736–4745 (2002)
129. S.E. Skrabalak, B.J. Wiley, M. Kim, E.V. Formo, Y. Xia, Nano Lett. **8**, 2077–2081 (2008)
130. H. Mao, J. Feng, X. Ma, C. Wu, X. Zhao, J. Nanoparticle Res. **14**, 2077–2081 (2012)
131. Y. Sun, B. Mayers, T. Herricks, Y. Xia, Nano Lett. **3**, 955–960 (2003)
132. Y. Xia, X. Xia, H.C. Peng, J. Am. Chem. Soc. **137**, 7947–7966 (2015)
133. Y. Xia, Y. Xiong, B. Lim, S.E. Skrabalak, Angew. Chemie Int. Ed. **48**, 60–103 (2009)
134. J. Jung, D. Seo, G. Park, S. Ryu, H. Song, J. Phys. Chem. C **114**, 12529–12534 (2010)
135. K. E. Korte, S.E. Skrabalak, Y. Xia, J. Mater. Chem. **18**, 437–441 (2008)
136. T. Cheng, Y. Zhang, W. Lai, Y. Chen, W. Huang, Chin. J. Chem. **33**, 147–151 (2015)
137. H. Mao, J. Feng, X. Ma, C. Wu, X. Zhao, J. Nanoparticle Res. 14, 887 (2012)

138. S. Coskun, B. Aksoy, H.E. Unalan, Cryst. Growth Des. **11**, 4963–4969 (2011)
139. L.D. Marks, Rep. Prog. Phys. **57**, 603 (1994)
140. W.A. Saidi, H. Feng, K.A. Fichthorn, J. Phys. Chem. C **117**, 1163–1171 (2013)
141. H. Feng, K. Fichthorn, Nano Lett. **12**, 997–1001 (2012)
142. B. Li, S. Ye, I. E. Stewart, S. Alvarez, B.J. Wiley, Nano Lett. **15**, 6722–6726 (2015)